

Corneal Epithelial Thickness Mapping by Fourier-Domain Optical Coherence Tomography in Normal and Keratoconic Eyes

Yan Li, PhD,¹ Ou Tan, PhD,¹ Robert Brass, MD,² Jack L. Weiss, MD,³ David Huang, MD, PhD¹

Objective: To map the corneal epithelial thickness with Fourier-domain optical coherence tomography (OCT) and to develop epithelial thickness-based variables for keratoconus detection.

Design: Cross-sectional observational study.

Participants: One hundred forty-five eyes from 76 normal subjects and 35 keratoconic eyes from 22 patients.

Methods: A 26 000-Hz Fourier-domain OCT system with 5- μm axial resolution was used. The cornea was imaged with a Pachymetry+Cpwr scan pattern (6-mm scan diameter, 8 radials, 1024 axial-scans each, repeated 5 times) centered on the pupil. Three scans were obtained at a single visit in a prospective study. A computer algorithm was developed to map the corneal epithelial thickness automatically. Zonal epithelial thicknesses and 5 diagnostic variables, including minimum, superior-inferior (S-I), minimum-maximum (MIN-MAX), map standard deviation (MSD), and pattern standard deviation (PSD), were calculated. Repeatability of the measurements was assessed by the pooled standard deviation. The area under the receiver operating characteristic curve (AUC) was used to evaluate diagnostic accuracy.

Main Outcome Measures: Descriptive statistics, repeatability, and AUC of the zonal epithelial thickness and diagnostic variables.

Results: The central, superior, and inferior epithelial thickness averages were $52.3 \pm 3.6 \mu\text{m}$, $49.6 \pm 3.5 \mu\text{m}$, and $51.2 \pm 3.4 \mu\text{m}$ in normal eyes and $51.9 \pm 5.3 \mu\text{m}$, $51.2 \pm 4.2 \mu\text{m}$, and $49.1 \pm 4.3 \mu\text{m}$ in keratoconic eyes. Compared with normal eyes, keratoconic eyes had significantly lower inferior ($P = 0.03$) and minimum ($P < 0.0001$) corneal epithelial thickness, greater S-I ($P = 0.013$), more negative MIN-MAX ($P < 0.0001$), greater MSD ($P < 0.0001$), and larger PSD ($P < 0.0001$). The repeatability of the zonal average, minimum, S-I, and MIN-MAX epithelial thickness variables were between 0.7 and 1.9 μm . The repeatability of MSD was better than 0.4 μm . The repeatability of PSD was 0.02 or better. Among all epithelial thickness-based variables investigated, PSD provided the best diagnostic power (AUC = 1.00). Using an PSD cutoff value of 0.057 alone gave 100% specificity and 100% sensitivity.

Conclusions: High-resolution Fourier-domain OCT mapped corneal epithelial thickness with good repeatability in both normal and keratoconic eyes. Keratoconus was characterized by apical epithelial thinning. The resulting deviation from the normal epithelial pattern could be detected with very high accuracy using the PSD variable.

Financial Disclosure(s): Proprietary or commercial disclosure may be found after the references. *Ophthalmology* 2012;xx:xxx © 2012 by the American Academy of Ophthalmology.



The human corneal epithelium covers the surface of the cornea, where it protects the eye and plays an important role in maintaining high optical quality. In diseases such as keratoconus, the thickness of the epithelium becomes altered to reduce corneal surface irregularity.¹ Therefore, the presence of an irregular stroma may be less measurable by frontal surface corneal topography. Analyzing the corneal epithelial and stromal thicknesses and shapes separately can facilitate the detection of the disease in its early stage.¹⁻³

Several methods, such as confocal microscopy, ultrasound, and optical coherence tomography (OCT), have been used to measure corneal epithelial thickness. Many studies used these methods to measure the average central epithelium thickness.⁴⁻⁷ Some used OCT to acquire peripheral epithelium thickness, but the number of points measured in the periphery was limited and the process was time consuming.⁸ Very high-frequency ultrasound can map the corneal epithelium and stromal thickness over a wide area.^{1,9-11} However, this method is inconvenient because it

requires immersion of the eye in a coupling fluid. Thus, a noncontact method of epithelial mapping is still needed.

Optical coherence tomography is a noncontact technique that is based on the principles of low-coherence interferometry.¹² The high axial resolution allows excellent delineation of corneal surfaces. Time-domain anterior segment OCT systems can provide pachymetry (corneal thickness) maps.^{13,14} Fourier-domain OCT, a newer generation of OCT, is capable of acquiring scans 10 to 100 times faster than time-domain OCT systems.^{15–20} This study developed software algorithms automatically to map corneal epithelial thickness in normal and keratoconic eyes imaged by a Fourier-domain OCT system. Epithelial thickness–based diagnostic variables also were developed to facilitate keratoconus detection.

Patients and Methods

Patients

Subjects of this cross-sectional observational study were recruited at Doheny Eye Institute at the University of Southern California, Los Angeles, California; Brass Eye Center, Latham, New York; Gordon & Weiss Vision Institute, San Diego, California; and the Casey Eye Institute at Oregon Health and Science University, Portland, Oregon. This study followed the tenets of the Declaration of Helsinki and was in accord with the Health Insurance Portability and Accountability Act of 1996. The study protocol was approved by the institutional review boards of the University of Southern California and the Oregon Health and Science University, and the Western Institutional Review Board. Written informed consent was obtained from all subjects, all of whom were 18 years of age or older.

Normal subjects were recruited from volunteers, patients seeking refractive surgery consultation, and patients seeking cataract surgery consultation. All had normal slit-lamp microscopy findings and normal topographic features. Normal subjects were divided into 2 groups for data analyzing purposes: normal group 1 and normal group 2. The keratoconic eyes included in this study were diagnosed clinically. Each had corrected distance visual acuity of 20/25 or worse and had at least 1 clinical sign other than the keratoconic appearance of the topography map (asymmetric bow-tie with skewed radial axis, central or inferior steep zone, or claw shape).^{21–23} The keratoconic slit-lamp findings included Munson's sign, Vogt's striae, Fleischer's ring, apical scar, apical thinning, or Rizutti's sign.²⁴ Eyes with late keratoconic changes such as corneal scars or hydrops were excluded because they have anomalous corneal epithelial findings and do not pose any diagnostic challenge. Contact lens wearers were not excluded from either group. None of the eyes had signs or history of other corneal disease, and none had undergone previous refractive or other ocular surgery.

Optical Coherence Tomography

A Fourier-domain OCT system (RTVue; Optovue, Inc., Fremont, CA) with a corneal adaptor module was used in this study. The system worked at 830-nm wavelength and had a scan speed of 26 000 axial scans per second. The depth resolution was 5 μm (full-width half-maximum) in tissue. The wide-angle (corneal long) adaptor lens used in this study provided a 6-mm-long scan width with a transverse resolution of 15 μm (focused spot size).¹⁷

A Pachymetry+Cpwr scan pattern (6-mm scan diameter, 8 radials, 1024 axial scans each, repeated 5 times) centered at the

pupil center was used to map the cornea (Fig 1). The RTVue corneal adaptor module software (software version 5.5) automatically processed the OCT scan to provide the pachymetry (corneal thickness) map and the minimum corneal thickness. Each eye was scanned 3 times within a single visit. Subjects were repositioned after each OCT scan.

Fourier-domain OCT image data were exported and processed with custom software. For each OCT scan, 5 repeated radial cross-sectional images on each meridian were registered and averaged. Next, the air–tear interface and the epithelium–Bowman's layer boundary were identified automatically with a computer algorithm by increased signal intensity at corresponding boundaries (Fig 2, available at <http://aojournal.org>).²⁵ Then, all boundaries detected were overlaid on the OCT image and were verified by visual inspection performed by one of the authors (Y.L.). Unless otherwise specified, sets of scans were excluded from the following data analysis if the visual inspection identified boundary segmentation error on any meridional cross-sectional image. Eyes were excluded from data analysis if they had fewer than 2 scans with valid epithelium detection.

Corneal epithelial thickness was measured as the distance between the air–tear and the epithelium–Bowman's interfaces perpendicular to the anterior surface at the point of measurement. An epithelial thickness profile was generated from each meridional cross-section.

Topography

Corneal topography was obtained by either Orbscan II (Bausch & Lomb, Houston, TX) or Pentacam (Oculus, Lynnwood, WA) for all study subjects. The steep keratometry reading of the simulated keratometry reading was recorded.

Epithelial Thickness Maps and Variables

A 6-mm-diameter epithelial thickness map was generated by interpolating epithelial thickness profiles calculated from each meridian. Only the central 5-mm-diameter map was used for calculating epithelial thickness–based variables.

Epithelial Thickness Map and Zonal Epithelial Thicknesses

The epithelial thickness map was divided into 3 zones by diameter and hemispheres: central 2 mm, superior 2 to 5 mm, and inferior 2 to 5 mm (Fig 3A). The average epithelial thicknesses of central, superior, and inferior zones were calculated. The average epithelial thickness maps of all normal subjects in normal group 1 were calculated for right and left eyes. The left eye maps were mirrored to the right eye to calculate the average map of both eyes. Similarly, the average epithelial thickness maps of all keratoconus subjects were calculated.

Epithelial Thinning, Focal Thinning, and Asymmetry

The minimum and maximum epithelial thicknesses were recorded, and the epithelial focal thinning was calculated as the difference between them (minimum–maximum [MIN-MAX]). Superior minus inferior asymmetry (superior–inferior [S-I]) was calculated by taking the difference between the average epithelial thicknesses of the superior and inferior zones.

Map Standard Deviation of the Epithelial Map

Map standard deviation (MSD) from the average value of a single epithelial thickness map was calculated as

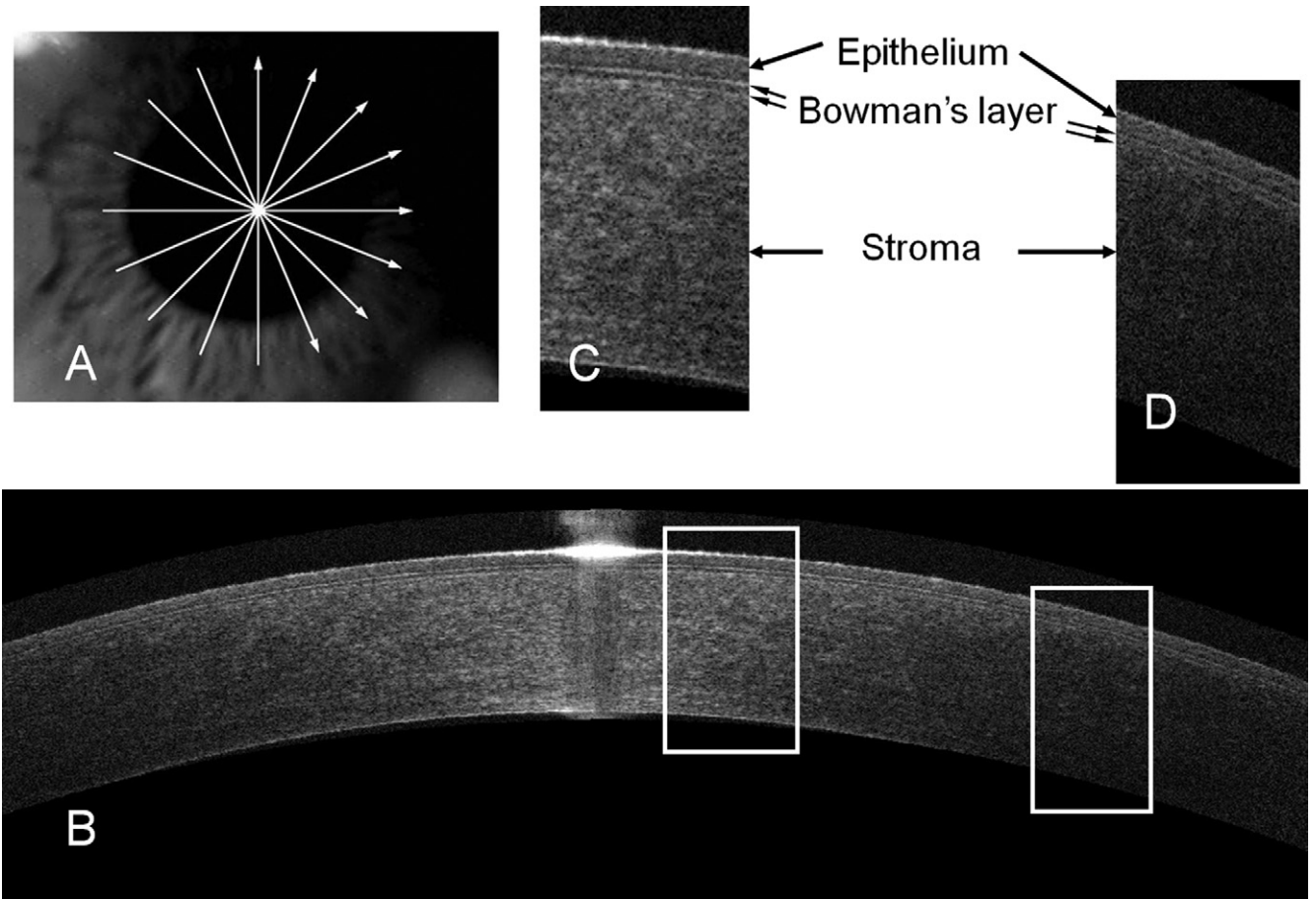


Figure 1. A, Pachymetry+OCT scan pattern consisting of 8 radial scans. B, Cross-sectional corneal optical coherence tomography (OCT) image (average of 5 repeated frames). C and D, Magnified sections of the OCT image shown in (B).

$$\text{MSD of the single epithelial map} = \sqrt{\frac{\sum_x \sum_y (\bar{T} - T(x, y))^2}{N}}, \quad [1]$$

where \bar{T} is the average epithelial thickness inside the 5-mm diameter area, and $T(x, y)$ was the epithelial thickness at map location (x, y) . The origin $(0, 0)$ was set to the map center. N was the total number of the map points inside the analytic zone ($\sqrt{x^2 + y^2} \leq 2.5 \text{ mm}$).

Epithelial Pattern Deviation Map

The epithelial pattern deviation map was calculated to show the difference between an individual epithelial pattern map and the average epithelial pattern map of normal subjects. The epithelial pattern map of the normal reference population P_N was calculated as

$$P_N(x, y) = T_N(x, y) / \bar{T}_N, \quad [2]$$

where T_N was the average epithelial thickness map of all normal subjects in normal group 1, and \bar{T}_N was the average thickness of map T_N . Similarly, the individual epithelial pattern map P was calculated as

$$P(x, y) = T(x, y) / \bar{T}, \quad [3]$$

where T was the individual epithelial thickness map, and \bar{T} was the average thickness of the map. The epithelial pattern deviation map (PD) was calculated as the difference between the individual epithelial pattern map (P) and the average normal epithelial pattern map (P_N):

$$PD(x, y) = P(x, y) - P_N(x, y). \quad [4]$$

Pattern Standard Deviation of the Epithelial Map

The pattern standard deviation (PSD) value was calculated from the pattern deviation map as

$$\text{PSD} = \sqrt{\frac{\sum_x \sum_y (PD(x, y))^2}{N}}, \quad [5]$$

where $PD(x, y)$ was the epithelial pattern deviation value at map location (x, y) . N was the total number of the map points inside the analytic zone.

Statistical Analysis

Normal subjects older than 65 years were excluded from data analysis to match the age of the keratoconus group. Descriptive statistics and other statistical analyses, including t tests, were performed using MedCalc software version 12.0 (MedCalc Software bvba, Mariakerke, Belgium). Mean \pm standard deviation values of each corneal epithelial thickness variable were calculated

Figure 3. Average epithelial thickness maps of (A–C) normal and (D–F) keratoconic eyes. Left column (A, D): all eyes were included with left eyes mirrored. Middle column (B, E): right eyes (OD) only. Right column (C, F): left eyes (OS) only. The red circles overlaid on the map had diameters of 2 and 5 mm. The color scale represents the thickness in micrometers. I = inferior; N = nasal; S = superior; T = temporal.

for both normal and keratoconus groups. Repeatability of epithelial thickness variables was assessed by the pooled standard deviation obtained from the multiple measurements of each eye. The normality of OCT variables was confirmed by a Kolmogorov-Smirnov test on the data set from which 1 eye was selected randomly from each normal subject.

To compare epithelial thickness variables measured in normal and keratoconic eyes, 2-tailed *t* tests were performed. If both eyes of a subject were involved in the study, a randomly selected eye was chosen for the *t* test to avoid the correlation between the 2 eyes from the same patient. *P* values less than 0.05 were considered statistically significant.

Receiver operating characteristic (ROC) curve analyses were performed to evaluate the diagnostic performance of the epithelial thickness variables. Normal subjects in normal group 2 and all keratoconic subjects were involved in the ROC curve analyses. If both eyes of a subject were involved in the study, a randomly selected eye was chosen for the ROC curve analyses. The area under the ROC curve (AUC) was calculated for each variable. A cutoff value of each variable was selected with the highest average of sensitivity and specificity. Corresponding sensitivity and specificity values were recorded. To assess the impact of segmentation errors on the diagnostic power of the epithelial thickness variables, separate ROC curve analyses were performed without excluding eyes and scans containing segmentation errors.

Results

Visual inspection confirmed that anterior corneal and epithelial boundary detection was satisfactory in 432 of 435 normal scans (99.3%) and in 107 of 114 keratoconic scans (93.9%). Three scans of normal eyes and 7 scans of keratoconic eyes were excluded from statistical analysis because of errors in boundary detection. Because the scans with segmentation errors occurred in different normal eyes, neither of those eyes was excluded. The keratoconic

boundary detection errors resulted in the loss of 3 eyes from the study. In one example of a boundary detection error, the algorithm mistakenly identified the Bowman's-stroma interface instead of the epithelium-Bowman's interface (Fig 4A, available at <http://aaojournal.org>). A possible reason for this type of segmentation error was the increased reflectivity of the epithelium associated with a decrease in contrast at the central Bowman's layer and stroma. In a second example of a boundary detection error, a clear epithelium-Bowman's interface reflectivity peak was absent be-

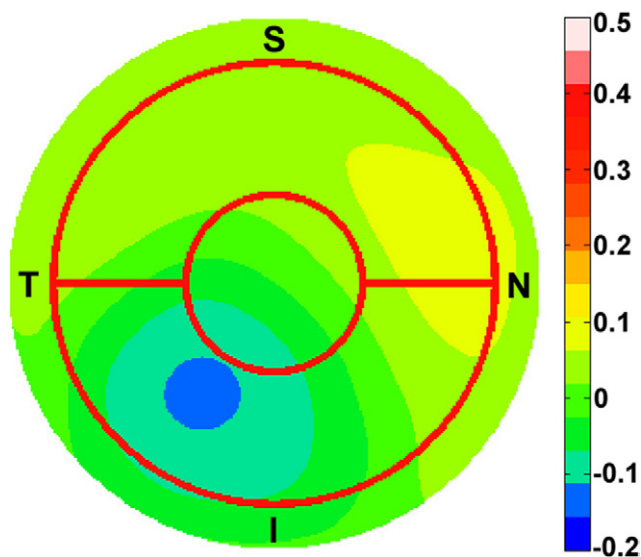


Figure 6. Average corneal epithelial thickness pattern deviation map of keratoconic eyes. All eyes were included with left eyes mirrored. The color scale represents pattern deviation with no units. I = inferior; N = nasal; S = superior; T = temporal.

Table 1. Repeatability of Corneal Epithelial Thickness Parameters by Pooled Standard Deviation

	No. of Eyes	Central	Superior	Inferior	Minimum	Superior-Inferior	Minimum-Maximum	Map Standard Deviation	Pattern Standard Deviation*
Normal	145	0.7	0.8	0.7	1.1	0.7	1.1	0.2	0.008
Keratoconus	35	1.0	1.0	1.0	1.8	1.3	1.9	0.4	0.020

*Pattern standard deviation was without units; all other variables had units of micrometers.

cause of the fragmentation of Bowman's layer (Fig 4B, available at <http://aojournal.org>).

Data were analyzed for 145 eyes of 76 normal subjects (29 men and 47 women) and 35 keratoconic eyes of 22 patients (12 men and 10 women). The average age of the normal subjects was 47.6 ± 13.9 years (range, 19–65 years) and 43.9 ± 12.3 years (range, 25–62 years) for keratoconus patients ($P = 0.25$). The steep keratometry reading averaged 44.3 ± 1.5 diopters (D; range, 41.0–47.8 D) for all normal subjects and 48.6 ± 4.4 D (range, 42.5–63.6 D) in the keratoconus group. The minimum corneal thickness was 530.4 ± 28.5 μm in normal eyes and 459.7 ± 50.5 μm in keratoconic eyes ($P < 0.0001$). The average base-10 logarithm of the minimum angle of resolution corrected distance visual acuity was 0.21 in keratoconic eyes, equivalent to 20/32.3 Snellen acuity (range, 20/25–20/200).

Fifty-four normal subjects were assigned to normal group 1 to calculate the normal reference population average epithelial thickness map (T_N) and the average normal epithelial pattern map (P_N). Twenty-two normal subjects were assigned to normal group 2 for ROC curve analyses. All 76 normal subjects were involved in all other statistical analyses.

The repeatability of epithelial thickness measurements in normal and keratoconic eyes is listed in Table 1. The repeatability of the zonal average, minimum, S-I, and MIN-MAX epithelial thickness variables were between 0.7 and 1.9 μm . The repeatability of MSD was better than 0.4 μm . The repeatability of PSD was 0.02 or better.

Significant differences in central and superior epithelial thickness values were not found between normal and keratoconic eyes ($P > 0.15$; Figure 3; Table 2). Compared with normal eyes, keratoconic eyes had a significantly thinner corneal epithelium inferiorly, lower minimum thickness, greater S-I, more negative MIN-MAX, greater MSD, and larger PSD (Tables 2 and 3).

The typical epithelial thickness pattern deviation map of a normal eye showed small deviations (color green and uniform pattern) from the average normal pattern map (Fig 5A, available at <http://aojournal.org>). In contrast, the pattern deviation map of a keratoconic eye contained large deviations (colors other than green and pattern uneven) from the average normal pattern map (Fig 5B, available at <http://aojournal.org>). The average pattern deviation map of all keratoconic eyes (left eyes mirrored) showed that on

average the epithelium was thinner inferotemporally and thicker supranasally in keratoconic eyes than in normal eyes (Fig 6).

For the variables minimum, MIN-MAX, and MSD, there was considerable overlap between the normal and keratoconic eyes (Fig 7). The least overlap occurred with PSD. Using the PSD cutoff value of 0.057 alone gave 100% specificity and 100% sensitivity (Table 4).

For ROC analyses excluding eyes and scans containing segmentation errors, PSD provided the best diagnostic power (AUC = 1.0; Table 4) among all of the epithelial thickness-based variables investigated in this study. The diagnostic power of other variables (Table 4) varied from poor (central, superior, and inferior zonal epithelial thicknesses), to fair (S-I), to good (minimum, MIN-MAX, and MSD). Even for ROC analyses including eyes and scans containing segmentation errors, the AUC of PSD was 1.00, and the AUCs of the other diagnostic variables changed less than 0.01. Figure 8 (available at <http://aojournal.org>) shows 1 normal, 1 mild keratoconus, and 1 advanced keratoconus case.

Discussion

Fourier-domain OCT instruments can provide scan speeds 10 to 100 times faster than time-domain OCT instruments.²⁶ The enhanced speeds minimize the effect of eye movements during data acquisition and also allow higher definition imaging because of denser axial scans in the same transverse scan length. The higher scan speed also facilitates frame averaging that suppresses speckle noise. The epithelium-Bowman's layer boundary is a relatively weak interface presented in corneal OCT images. In this study, the epithelial boundary was enhanced by acquiring 5 repeated images and averaging them after the registration. The averaged image had a higher signal-to-noise ratio than the single frame. Moreover, the Fourier-domain OCT system used in this study had an axial resolution of 5 μm , which is 2 to 3 times higher than that of time-domain instruments used in previous studies.^{6,27–29} Not only does the higher resolution and higher speed of Fourier-domain OCT improve image quality, it also makes the automated corneal epithelial thickness mapping possible.

The corneal epithelium is the first cellular layer of the human cornea and protects the eye. Accurate and reproducible measurement of corneal epithelial thickness provides important information for assessing corneal remodeling after refractive surgeries such as photorefractive keratectomy and LASIK.³⁰ Moreover, deviations from normal epithelial thickness could be an early sign of keratoconus.¹ Many efforts had been made to measure the corneal epithelial thickness (Table 5). Li et al,⁴ Erie et al,⁵ and Patel et al³¹ reported central epithelial thicknesses of 41 to 50.6 μm in normal corneas measured by confocal microscopy. Their

Table 2. Epithelial Map Zonal Thickness Variables

	No. of Eyes	Central	Superior	Inferior	Minimum
Normal	145	52.3 \pm 3.6	49.6 \pm 3.5	51.2 \pm 3.4	46.0 \pm 4.3
Keratoconus	35	51.9 \pm 5.3	51.2 \pm 4.2	49.1 \pm 4.3	40.0 \pm 6.0
<i>P</i> value (<i>t</i> test)*		0.42	0.15	0.03	<0.0001

Descriptive statistics are in micrometers.

*The fellow eye was excluded from *t* tests to eliminate the correlation between the 2 eyes of a subject.

Table 3. Epithelial Map Uniformity Indices

	No. of Eyes	Superior-Inferior	Minimum-Maximum	Map Standard Deviation	Pattern Standard Deviation*
Normal	145	-1.6 ± 1.8	-8.8 ± 3.5	2.1 ± 0.8	0.030 ± 0.009
Keratoconus	35	2.1 ± 5.4	-18.7 ± 8.0	4.7 ± 2.0	0.105 ± 0.030
P value (t test) [†]		0.013	<0.0001	<0.0001	<0.0001

*Pattern standard deviation was without units; descriptive statistics of all other variables are in micrometers.

[†]The fellow eye was excluded from t tests to eliminate the correlation between the 2 eyes of a subject.

measurements, which excluded the pre-corneal tear film thickness, were thinner than the central epithelial thickness of $52.3 \pm 3.6 \mu\text{m}$ in normal eyes obtained in the present study. The current measurements included the thickness of tear film, approximately $3 \mu\text{m}$,³² which probably accounts for the difference. Reinstein et al^{1,9,10} pioneered corneal epithelial thickness mapping using very high-frequency ultrasound over the entire corneal surface. The central epithelial thickness of normal eyes from their study, which excluded the tear film, was $53.4 \pm 4.6 \mu\text{m}$.⁹ Their research also demonstrated that corneal epithelium was thicker inferiorly than superiorly in the normal corneas.⁹ The present findings (S-I mean difference, $-1.6 \mu\text{m}$) agreed with their results.

Optical coherence tomography is a noncontact imaging method with high axial resolution. Several investigators used time-domain OCT systems to measure corneal epithelial thickness. Among them, Sin and Simpson,⁶ Haque et al,²⁸ and Feng and Simpson²⁹ reported central corneal epithelial thicknesses of 52 to $54.7 \mu\text{m}$ in normal eyes, values that are very close to the present measurements. In contrast,

Wang et al,²⁷ also using a time-domain system, reported a thicker value, $59.9 \pm 5.9 \mu\text{m}$. Recently, Tao et al³³ used a custom-built Fourier-domain OCT to measure central epithelial thickness in normal subjects. Their finding of $52.5 \pm 2.4 \mu\text{m}$ was similar to the present finding. Francoz et al³⁴ used a commercial Fourier-domain OCT to measure central epithelial thickness in young adults (<40 years) and middle-age adults (>40 years) and found that the thickness was similar, approximately $48.5 \mu\text{m}$, for the 2 groups. They excluded the pre-corneal tear film from the thickness determinations, which probably explains why their values were thinner than those measured in the current study.

Keratoconus is a degenerative condition in which the cornea progressively displays an irregular, cone-like shape. It is an important contraindication for refractive surgeries such as LASIK and photorefractive keratectomy. Undetected keratoconus can result in accelerated, progressive keratoectasia and unpredictable outcomes after the surgery.³⁵⁻⁴⁰ Haque et al²⁸ reported that the central epithelial thickness in individuals with keratoconus was $4.7 \mu\text{m}$ thin-

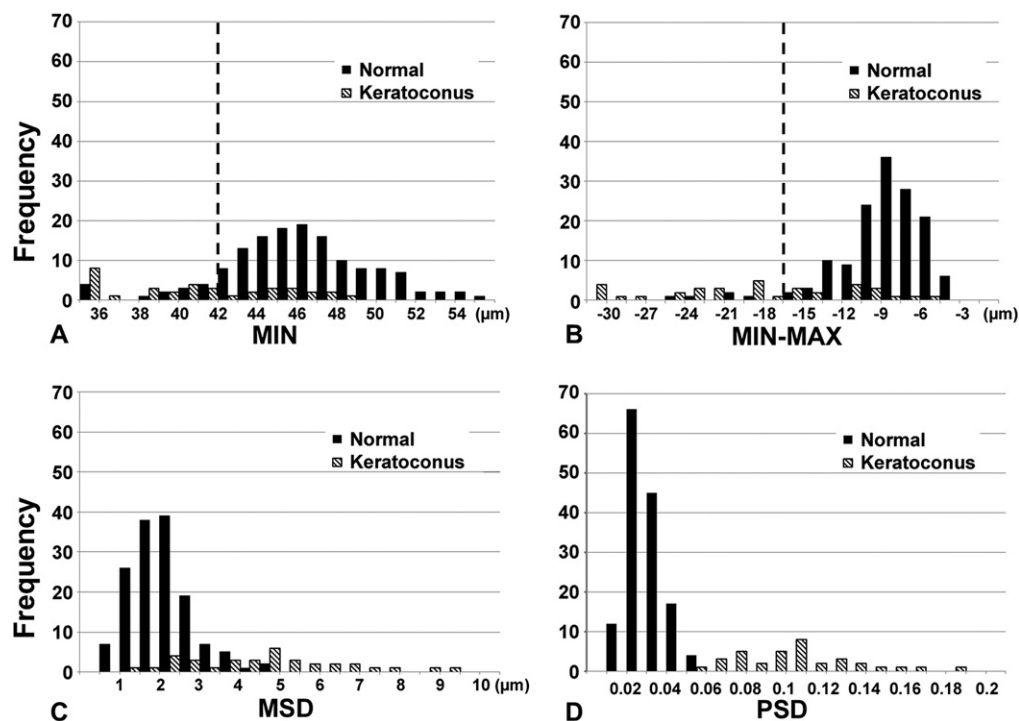


Figure 7. Histograms showing 4 corneal epithelial thickness-based variables. A, Minimum (MIN). B, Minimum-maximum (MIN-MAX). C, Map standard deviation (MSD). D, Pattern standard deviation (PSD). Dashed lines indicated optimized cutoff values of the variables.

Table 4. Cutoff Criterion, Sensitivity, Specificity, and Area under the Receiver Operating Characteristic Curve of Epithelial Thickness Variables

	Central	Superior	Inferior	Minimum	Superior-Inferior	Minimum-Maximum	Map Standard Deviation	Pattern Standard Deviation*
Criterion	<48.4	>51.9	<48.1	<41.8	>0.0	<-16.3	>3.6	>0.057
Sensitivity	31.8	50.0	31.8	63.6	68.2	68.2	72.7	100
Specificity	100	72.7	95.5	95.5	81.8	95.5	95.5	100
AUC	0.61	0.57	0.64	0.84	0.73	0.88	0.89	1.00
95% CI	0.45–0.75	0.41–0.72	0.48–0.78	0.69–0.93	0.58–0.86	0.75–0.96	0.76–0.97	0.92–1.0

AUC = area under the receiver operating characteristic curve; CI = confidence interval.

*Pattern standard deviation was without units; criteria of all other variables are in micrometers.

ner than the control thickness. Reinstein et al¹ found that the central epithelial thickness in keratoconic eyes, $45.7 \pm 5.9 \mu\text{m}$, was significantly thinner than in normal eyes. In the present study, a statistically significant difference was not detected. One possibility was that the ectasia usually was located inferotemporally in the keratoconic corneas. The ultrasound scan in the Reinstein et al study was centered on corneal vertex, which is shifted inferotemporally in keratoconus. The OCT scan in the present study was centered on the pupil, which was not displaced by the cone location. However, the minimum corneal epithelial thickness in keratoconic eyes, $40.0 \pm 6.0 \mu\text{m}$, was significantly thinner than that of normal eyes, $46.0 \pm 4.3 \mu\text{m}$. In addition to their interesting finding that epithelial thinning occurred at the apex of the cone, Reinstein et al also showed that the zone of epithelial thinning was surrounded by an annulus of thicker epithelium.

Previously, a mathematical model was developed to describe epithelial smoothing in response to corneal contour change after laser refractive surgery.³⁰ Reinstein et al¹ indicated that the epithelium seems to remodel to eliminate or reduce the bulging of the anterior stromal surface. Both suggest that epithelial smoothing may play an important role in reducing the irregularity of the anterior stromal surface in keratoconus. Moreover, greater S-I and MIN-

MAX epithelial thickness differences, greater MSD, and larger PSD were observed. All demonstrated that corneal epithelial thickness variation was increased significantly in keratoconic eyes.

Several corneal epithelial thickness-based variables developed in this study showed good (minimum, AUC = 0.84; MIN-MAX, AUC = 0.88; MSD, AUC = 0.89) to excellent (PSD, AUC = 1.00) diagnostic power in differentiating keratoconic from normal eyes. By far, PSD was the best variable. With a cutoff value of 0.057, PSD alone gave 100% specificity and 100% sensitivity. These variables could be applied to epithelial thickness maps from other imaging systems as well (for example, very high-frequency ultrasound). Moreover, these variables may be useful for detecting forme fruste keratoconus (or subclinical keratoconus). Further studies are needed to evaluate the performance of these variables in forme fruste keratoconus detection.

One limitation of the technology used in this study is that the RTVue corneal adaptor module OCT provides pachymetric and epithelial thickness maps of only the central 6-mm diameter of the cornea. The 6-mm map size may be sufficient for planning myopic LASIK and photorefractive keratectomy because the central corneal tissue is ablated most for myopic refractive surgery procedures. It may be sufficient for keratoconus screening because a previous study showed that the cone apex was located inside the central 5-mm diameter of the cornea in the vast majority of keratoconic eyes.⁴¹ However, the 6-mm map size is a limitation for diseases involving the peripheral cornea, such as pellucid marginal degeneration. Moreover, a full ring of thicker epithelium surrounding the localized corneal thinning, as presented by Reinstein et al, was not observed. A larger epithelial map size may facilitate further comparison on epithelial thickness map patterns.

Another limitation of the technology is segmentation error by the automated epithelial boundary detection algorithm in a small percentage of scans. These failures tend to occur in keratoconic eyes. The errors were associated with higher central epithelial reflectivity or reduced contrast between the Bowman's layer and stroma. The higher epithelial reflectivity could be caused by chronic rubbing from rigid gas permeable contact lens wear. The loss of a distinct reflectivity peak in Bowman's layer in some keratoconic eyes could be explained by thinning or fragmentation of

Table 5. Central Corneal Epithelial Thickness Reported by Previous Investigators

Study	Normal (μm)	Keratoconus (μm)	Instrument Used
Li et al ⁴	$50.6 \pm 3.9^*$		Confocal microscopy
Erie et al ⁵	$46 \pm 5^*$		Confocal microscopy
Patel et al ³¹	$41 \pm 4^*$		Confocal microscopy
Reinstein et al ^{1,9}	$53.4 \pm 4.6^*$	$45.7 \pm 5.9^*$	Very high-frequency ultrasound
Wang et al ²⁷	59.9 ± 5.9		Time-domain OCT
Sin et al ⁶	52 ± 3		Time-domain OCT
Haque et al ²⁸	52.9 ± 4.1	48.2 ± 5.5	Time-domain OCT
Feng et al ²⁹	54.7 ± 1.9		Time-domain OCT
Tao et al ³³	52.5 ± 2.4		Fourier-domain OCT
Francoz et al ³⁴	$48.3 \pm 2.9^*$		Fourier-domain OCT
Present study	52.3 ± 3.6	51.9 ± 5.3	Fourier-domain OCT

OCT = optical coherence tomography.

*Pre-corneal tear thickness was excluded.

Bowman's layer, which occurs in this disease. Because low contrast between the epithelium, Bowman's layer, and anterior stroma are associated with these segmentation errors, an automated grading system could be developed based on the contrast to warn users when the reliability of the epithelial thickness measurement is low. Nevertheless, ROC analyses showed that segmentation error did not affect the discrimination between normal and keratoconic eyes in this study. One reason is that the segmentation error was small, no more than the thickness of the Bowman's layer.³³ Also, the segmentation error typically occurred only in a small part of the 8 cross-sectional meridional scans. Thus, for the purpose keratoconus detection, these small segmentation errors do not present a practical problem. However, the reliability of epithelial thickness mapping in other situations where the contrast between the epithelium and subjacent layers are altered, such as eyes that have undergone phototherapeutic keratectomy, requires further study before this method can be applied confidently.

Rigid gas permeable contact lens wearing could produce apical epithelial thinning. This thinning effect may be combined with the epithelial thinning resulting from keratoconus in keratoconic subjects wearing rigid gas permeable contact lenses. It is a limitation of the present study that contact lens history was not collected and the time between contact lens removal and examination was not recorded. This deserves more attention in future studies. Nevertheless, the best diagnostic variable of this study—PSD—had 100% specificity and sensitivity with mixed subjects of contact lens users and non-users. The specificity and sensitivity would have remained 100% if the ROC analysis had been performed separating the contact lens users and nonusers.

In summary, high-resolution Fourier-domain OCT was used to map corneal epithelial thickness successfully, with good repeatability in both normal and keratoconic eyes. Keratoconus was characterized by apical epithelial thinning. The resulting deviation from the normal epithelial pattern could be detected with very high accuracy using the PSD variable.

Acknowledgment. The authors thank Dr. Qienyuan Zhou for coordinating study data collection, Dr. Xinbo Zhang for consultation in statistics, and Dr. Maolong Tang for consultation on corneal topography.

References

1. Reinstein DZ, Gobbe M, Archer TJ, et al. Epithelial, stromal, and total corneal thickness in keratoconus: three-dimensional display with Artemis very-high frequency digital ultrasound. *J Refract Surg* 2010;26:259–71.
2. Reinstein DZ, Archer TJ, Gobbe M. Corneal epithelial thickness profile in the diagnosis of keratoconus. *J Refract Surg* 2009;25:604–10.
3. Reinstein DZ, Archer TJ, Gobbe M. Stability of LASIK in topographically suspect keratoconus confirmed non-keratoconic by Artemis VHF digital ultrasound epithelial thickness mapping: 1-year follow-up. *J Refract Surg* 2009;25:569–77.
4. Li HF, Petroll WM, Moller-Pedersen T, et al. Epithelial and corneal thickness measurements by in vivo confocal microscopy through focusing (CMTF). *Curr Eye Res* 1997;16:214–21.
5. Erie JC, Patel SV, McLaren JW, et al. Effect of myopic laser in situ keratomileusis on epithelial and stromal thickness: a confocal microscopy study. *Ophthalmology* 2002;109:1447–52.
6. Sin S, Simpson TL. The repeatability of corneal and corneal epithelial thickness measurements using optical coherence tomography. *Optom Vis Sci* 2006;83:360–5.
7. Wang J, Fonn D, Simpson TL, Jones L. The measurement of corneal epithelial thickness in response to hypoxia using optical coherence tomography. *Am J Ophthalmol* 2002;133:315–9.
8. Haque S, Jones L, Simpson T. Thickness mapping of the cornea and epithelium using optical coherence tomography. *Optom Vis Sci* 2008;85:E963–76.
9. Reinstein DZ, Archer TJ, Gobbe M, et al. Epithelial thickness in the normal cornea: three-dimensional display with Artemis very high-frequency digital ultrasound. *J Refract Surg* 2008;24:571–81.
10. Reinstein DZ, Archer TJ, Gobbe M, et al. Epithelial thickness after hyperopic LASIK: three-dimensional display with Artemis very high-frequency digital ultrasound. *J Refract Surg* 2010;26:555–64.
11. Reinstein DZ, Silverman RH, Raevsky T, et al. Arc-scanning very high-frequency digital ultrasound for 3D pachymetric mapping of the corneal epithelium and stroma in laser in situ keratomileusis. *J Refract Surg* 2000;16:414–30.
12. Huang D, Swanson EA, Lin CP, et al. Optical coherence tomography. *Science* 1991;254:1178–81.
13. Li Y, Shekhar R, Huang D. Corneal pachymetry mapping with high-speed optical coherence tomography. *Ophthalmology* 2006;113:792–9.
14. Li EY, Mohamed S, Leung CK, et al. Agreement among 3 methods to measure corneal thickness: ultrasound pachymetry, Orbscan II, and Visante anterior segment optical coherence tomography. *Ophthalmology* 2007;114:1842–7.
15. Christopoulos V, Kagemann L, Wollstein G, et al. In vivo corneal high-speed, ultra high-resolution optical coherence tomography. *Arch Ophthalmol* 2007;125:1027–35.
16. Ko TH, Fujimoto JG, Duker JS, et al. Comparison of ultra-high- and standard-resolution optical coherence tomography for imaging macular hole pathology and repair. *Ophthalmology* 2004;111:2033–43.
17. Li Y, Tang ML, Zhang XB, et al. Pachymetric mapping with Fourier-domain optical coherence tomography. *J Cataract Refract Surg* 2010;36:826–31.
18. Sarunic MV, Asrani S, Izatt JA. Imaging the ocular anterior segment with real-time, full-range Fourier-domain optical coherence tomography. *Arch Ophthalmol* 2008;126:537–42.
19. Wojtkowski M, Leitgeb R, Kowalczyk A, et al. In vivo human retinal imaging by Fourier domain optical coherence tomography. *J Biomed Opt* 2002;7:457–63.
20. Yasuno Y, Madjarova VD, Makita S, et al. Three-dimensional and high-speed swept-source optical coherence tomography for in vivo investigation of human anterior eye segments. *Opt Express* [serial online] 2005;13:10652–64. Available at: <http://www.opticsinfobase.org/oe/abstract.cfm?uri=oe-13-26-10652>. Accessed June 2, 2012.
21. Binder PS, Lindstrom RL, Stulting RD, et al. Keratoconus and corneal ectasia after LASIK. *J Refract Surg* 2005;21:749–52.
22. Jafri B, Li X, Yang H, Rabinowitz YS. Higher order wavefront aberrations and topography in early and suspected keratoconus. *J Refract Surg* 2007;23:774–81.
23. Lee BW, Jurkunas UV, Harissi-Dagher M, et al. Ectatic disorders associated with a claw-shaped pattern on corneal topography. *Am J Ophthalmol* 2007;144:154–6.

24. Rabinowitz YS. Keratoconus. *Surv Ophthalmol* 1998;42:297–319.
25. Li Y, Tan O, Huang D. Normal and keratoconic corneal epithelial thickness mapping using Fourier-domain optical coherence tomography. In: Weaver JB, Molthen RC, eds. *Medical Imaging 2011: Biomedical Applications in Molecular, Structural, and Functional Imaging*. Bellingham, WA: SPIE; 2010:796508.
26. Fujimoto J, Huang D. Introduction to optical coherence tomography. In: Huang D, Duker J, Fujimoto J, et al, eds. *Imaging the Eye from Front to Back with RTVue Fourier-Domain Optical Coherence Tomography*. Thorofare, NJ: Slack; 2010:1–21.
27. Wang J, Thomas J, Cox I, Rollins A. Noncontact measurements of central corneal epithelial and flap thickness after laser in situ keratomileusis. *Invest Ophthalmol Vis Sci* 2004;45:1812–6.
28. Haque S, Simpson T, Jones L. Corneal and epithelial thickness in keratoconus: a comparison of ultrasonic pachymetry, Orbscan II, and optical coherence tomography. *J Refract Surg* 2006;22:486–93.
29. Feng Y, Simpson TL. Corneal, limbal, and conjunctival epithelial thickness from optical coherence tomography. *Optom Vis Sci* 2008;85:E880–3.
30. Huang D, Tang M, Shekhar R. Mathematical model of corneal surface smoothing after laser refractive surgery. *Am J Ophthalmol* 2003;135:267–78.
31. Patel SV, Erie JC, McLaren JW, Bourne WM. Confocal microscopy changes in epithelial and stromal thickness up to 7 years after LASIK and photorefractive keratectomy for myopia. *J Refract Surg* 2007;23:385–92.
32. Azartash K, Kwan J, Paugh JR, et al. Pre-corneal tear film thickness in humans measured with a novel technique. *Mol Vis* [serial online] 2011;17:756–67. Available at: <http://www.molvis.org/molvis/v17/a86/>. Accessed June 2, 2012.
33. Tao A, Wang J, Chen Q, et al. Topographic thickness of Bowman's layer determined by ultra-high resolution spectral domain-optical coherence tomography. *Invest Ophthalmol Vis Sci* 2011;52:3901–7.
34. Francoz M, Karamoko I, Baudouin C, Labbe A. Ocular surface epithelial thickness evaluation with spectral-domain optical coherence tomography. *Invest Ophthalmol Vis Sci* 2011;52:9116–23.
35. Amoils SP, Deist MB, Gous P, Amoils PM. Iatrogenic keratectasia after laser in situ keratomileusis for less than -4.0 to -7.0 diopters of myopia. *J Cataract Refract Surg* 2000;26:967–77.
36. Binder PS, Lindstrom RL, Stulting RD, et al. Keratoconus and corneal ectasia after LASIK [letter]. *J Cataract Refract Surg* 2005;31:2035–8.
37. Krachmer JH, Feder RS, Belin MW. Keratoconus and related noninflammatory corneal thinning disorders. *Surv Ophthalmol* 1984;28:293–322.
38. Randleman JB, Russell B, Ward MA, et al. Risk factors and prognosis for corneal ectasia after LASIK. *Ophthalmology* 2003;110:267–75.
39. Seiler T, Quirke AW. Iatrogenic keratectasia after LASIK in a case of forme fruste keratoconus. *J Cataract Refract Surg* 1998;24:1007–9.
40. Randleman JB, Woodward M, Lynn MJ, Stulting RD. Risk assessment for ectasia after corneal refractive surgery. *Ophthalmology* 2008;115:37–50.
41. Tang M, Shekhar R, Miranda D, Huang D. Characteristics of keratoconus and pellucid marginal degeneration in mean curvature maps. *Am J Ophthalmol* 2005;140:993–1001.

Footnotes and Financial Disclosures

Originally received: December 12, 2011.

Final revision: June 13, 2012.

Accepted: June 14, 2012.

Available online: ●●●.

Manuscript no. 2011-1777.

¹ Center for Ophthalmic Optics and Lasers, Casey Eye Institute and Department of Ophthalmology, Oregon Health and Science University, Portland, Oregon.

² Brass Eye Center, Latham, New York.

³ Gordon & Weiss Vision Institute, San Diego, California.

Presented in part at: American Society of Cataract and Refractive Surgery Annual Meeting, April 2010, Boston, Massachusetts; and Association for Research in Vision and Ophthalmology Annual Meeting, May 2010, Fort Lauderdale, Florida.

Financial Disclosure(s):

The author(s) have made the following disclosure(s):

Yan Li received travel support, research grant support, patent royalty from Optovue, Inc., Fremont, CA; Ou Tan received research grant support,

patent royalty from Optovue, Inc.; Robert Brass receives speaker honoraria from Optovue, Inc.; David Huang received stock options, patent royalty, travel support and research grant support from Optovue, Inc. David Huang receives royalties from the Massachusetts Institute of Technology derived from an optical coherence tomography patent licensed to Carl Zeiss Meditec, Inc. (Dublin, CA).

These potential conflicts of interest have been reviewed and managed by Oregon Health and Science University.

Supported by the National Institutes of Health, Bethesda, Maryland (grant no.: R01EY018184); a research grant from Optovue, Inc., Fremont, California; and an unrestricted grant to Casey Eye Institute from Research to Prevent Blindness, Inc., New York, New York.

Correspondence:

Yan Li, PhD, Casey Eye Institute, Oregon Health and Science University, 3375 SW Terwilliger Boulevard, Portland, OR 97239. E-mail: liyan@ohsu.edu.